Turner, *Annu. Rev. Cell Biol.* 4, 487 (1988); B. Geiger, T. Volk, T. Volberg, R. Bendori, *J. Cell Sci. Suppl.* 8, 251 (1987).
4. R. O. Hynes, *Cell* 69, 11 (1992).
5. D. Hanein, H. Sabanay, L. Addadi, B. Geiger, *J. Cell Sci.* 104, 257 (1993).
6. Crystal faces are described by a set of indices (*hkl*) that unequivocally define the orientation of the face relative to the crystallographic axes *a*, *b*, and *c* of the structure. The notation {*h,k,l*}, such as {011}, includes a set of faces—$(01\bar{1})$, $(0\bar{1}1)$, and $(0\bar{1}\bar{1})$—that are identical to (011) because they are related to it by the symmetry of these crystals.
7. G. K. Ambady, *Acta Crystallogr. Sect. B* 24, 1548 (1968).
8. D. Hanein, B. Geiger, L. Addadi, *Langmuir* 9, 1058 (1993).
9. Many adhesive proteins present in the extracellular matrices and in the blood contain the sequence RGD as their major cell recognition site. The RGD sequences of each of the adhesive proteins are recognized by at least one member of structurally related receptors of the integrin superfamily. The synthetic peptides, containing the RGD sequence, inhibit extracellular matrix-mediated cell adhesion.
10. Routinely, cell growth was performed in the presence of 10% fetal bovine serum, saturated with respect to the particular crystal used (saturated complete medium).
11. A6 cells were seeded on a mixture of calcium (*S,S*)- and (*R,R*)-tartrate tetrahydrate crystals in 5.5-cm Falcon (Plymouth, United Kingdom) culture dishes. The crystals were homogeneous in size, and the starting weight of each fraction was ~60.0 mg. After 10 min, the cells were fixed with 2% glutaraldehyde in 0.1 M cacodylate buffer, pH 7.2, containing 5 mM $CaCl_2$. The dishes were rinsed four times, postfixed with 1% osmium tetroxide in the same buffer, and dried. The fixation kept the cells in situ and enhanced contrast. The crystals on which cells were observed were manually separated from others under a Zeiss (Oberkochen, Germany) stereomicroscope, 80× magnification. The selected cell-coated crystals (16.2 mg) were dissolved in 1 ml of 1 M HCl, and the optical activity of the solution was measured with a Perkin-Elmer 141 polarimeter. The optical activity of the solution was $\alpha = +0.104$, $[\alpha]_D = +6.30$, corresponding to (*R,R*) tartaric acid of 86.2% enantiomeric purity $\{[\alpha]_D = +7.3$ for pure calcium (*R,R*)-tartrate tetrahydrate in 1 M HCl$\}$. The experiment was repeated, yielding $[\alpha]_D = +6.06$, corresponding to (*R,R*) tartaric acid of 83% enantiomeric purity.
12. L. Pasteur, *Ann. Chim. Phys.* **xxiv**, 442 (1848).
13. B. Geiger, D. Salomon, M. Takeichi, R. O. Hynes, *J. Cell Sci.* 103, 943 (1992).
14. A. S. G. Curtis and P. Clark, *Crit. Rev. Biocompat.* 5, 343 (1990).
15. We thank K. Ben-Ari, a high school student who performed her final class project in our laboratory, for motivating with her presence the execution of this work. We thank our colleagues M. Lahav and S. Weiner for critically reading the manuscript. B.G. holds the E. Neter Chair for Cell and Tumor Biology. L.A. is incumbent of the Patrick E. Gorman Chair of Biological Ultrastructure. This work is supported in part by the Kimmelman Center for Structural Biology, a grant from the Minerva Foundation, Munich, Germany (B.G.), and the Anniversary Fund of the Austrian National Bank.

18 October 1993; accepted 12 January 1994

Direct Observation of Microscopic Inhomogeneities with Energy-Dispersive Diffraction of Synchrotron-Produced X-rays

E. F. Skelton, A. R. Drews, M. S. Osofsky, S. B. Qadri, J. Z. Hu,
T. A. Vanderah,* J. L. Peng, R. L. Greene

Evidence of structural inhomogeneities in two high–transition-temperature superconductors, $YBa_2Cu_3O_{7-\delta}$ and $Nd_{2-x}Ce_xCuO_{4-y}$, is presented. When samples were illuminated by highly collimated x-rays produced on a synchrotron wiggler, small changes in the lattice were detected over a spatial scale of 10 micrometers. These changes are interpreted as evidence of variations in the oxygen content in one case and in the cerium content in the other; both affect the superconducting properties. The existence of such structural inhomogeneities brings into question whether exotic experimental results obtained from superconducting materials with high transition temperatures actually reflect intrinsic properties.

High-temperature superconductors (HTS) still present many mysteries in both their chemical properties and the mechanism of superconductivity. One of the few characteristics that is universally accepted is that their coherence lengths, ξ, are short (on the order of tens of angstroms). Because ξ is the decay distance of the superconducting order parameter, sample inhomogeneities, even in single crystals, strongly affect the measured superconductive properties of the system. These inhomogeneities are undoubtedly the source of many of the unusual properties that have been reported in HTS. In this report, we present direct structural evidence of microscopic oxygen and cation inhomogeneities in crystals of HTS.

Standard diffraction techniques with conventional x-ray sources are the classic method for obtaining structural information. This information is limited to a surface region of the sample, as defined by the penetration depth of the radiation. This depth varies with photon energy and the atomic number of the elements in the sample. Typical skin depths are on the order of a few micrometers. Spot sizes are determined, in part, by the degree to which the radiation from an x-ray generator can be collimated, while retaining an adequate number of photons in the beam to perform the measurement. Typical beam diameters are on the order of millimeters. Neutron diffraction typically requires samples of millimeter dimensions or larger, and although electron beam cross sections can be reduced to less than a micrometer, their penetrating power is limited. However, with the use of high energy photons from a synchrotron wiggler, with its concomitant low angular dispersion, materials can be probed roughly two orders of magnitude deeper with x-ray beams that are <100 μm^2 in cross-sectional area. Using such an arrangement, we have detected small compositional variances on spatial scales of a few tens of micrometers.

Experiments were performed on a $YBa_2Cu_3O_{7-\delta}$ single crystal to determine compositional uniformity. The *c* axis length of the orthorhombic unit cell of bulk samples of these compounds is a reliable indicator of the oxygen content, 7 − δ (*1*)

$$7 - \delta = 74.49 - 5.787\,c \qquad (1)$$

where *c* is in angstroms. The $YBa_2Cu_3O_{7-\delta}$ crystals were grown from an off-stoichiometric flux in a zirconia crucible as described in detail elsewhere (*1*). The crystal selected for this study was mechanically detwinned (*2*). Optical microscopic analysis after detwinning showed the crystal to be almost entirely twin-free, and x-ray studies on a four-circle diffractometer showed no evidence of twinning. On the basis of ac-susceptibility measurements, the transition temperature T_c had an onset of 93 K and a width less than 0.5 K.

The crystal was in the approximate shape of a rectangular solid, with dimensions 470 μm by 340 μm by 75 μm. The $[0,0,\ell]$ reciprocal lattice vector was normal to the largest face, and the longest edge was approximately parallel to the *b* axis. The crystal was mounted on an ω,χ circle (angles ω and χ measure the rotational motion of the sample about vertical and horizontal axes, respectively), contained on an *xyz*-translation stage on beamline X17C at the National Synchrotron Light Source (NSLS), Brookhaven National Laboratory, and was

---

E. F. Skelton, A. R. Drews, M. S. Osofsky, S. B. Qadri, Condensed Matter and Radiation Sciences Division and Materials Science and Technology Division, Naval Research Laboratory, Washington, DC 20375–5000, USA.
J. Z. Hu, Geophysical Laboratory and Center for High Pressure Research, Carnegie Institution of Washington, Washington, DC 20015–1305, USA.
T. A. Vanderah, Chemistry Division, Research Department, Naval Air Warfare Center, Weapons Division, China Lake, CA 93555, USA.
J. L. Peng and R. L. Greene, Center for Superconductivity Research, Department of Physics, University of Maryland, College Park, MD 20742, USA.

*Present address: Ceramics Division National Institute of Standards and Technology, Gaithersburg, MD 20882, USA.

aligned for the $(0,0,\ell)$ class of reflections. The longest edge was aligned parallel to the z axis (vertical axis) when $\chi = 0°$. The x axis is taken to be parallel to the on-going beam, and the y axis is orthogonal to x and z. The crystal was illuminated with unfiltered, polychromatic radiation emerging from the wiggler magnet (operated at 5.2 T) that was restricted by an aperture 5 μm wide and 10 μm high. The scattered x-rays were analyzed at a fixed diffraction angle, 2θ, of 13.002° as a function of energy with an intrinsic Ge energy-sensitive detector. Once the experiment was started, only the sample moved; all other components of the system remained stationary.

Diffraction spectra were collected as a function of z in steps, ranging in size from 2 to 100 μm, from the upper edge to the lower edge of the crystal. At each position, the $(0,0,\ell)$ peaks were automatically centered in ω and χ and then the spectrum was recorded (Fig. 1). The length of the c axis can be calculated from the measured energy of any of the $(0,0,\ell)$ peaks, E_ℓ, with Bragg's Law

$$c = \frac{\ell\kappa}{2E_\ell \sin\theta} \qquad (2)$$

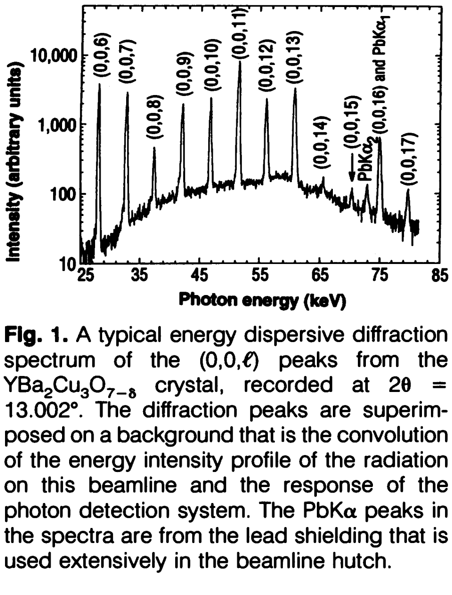

Fig. 1. A typical energy dispersive diffraction spectrum of the $(0,0,\ell)$ peaks from the $YBa_2Cu_3O_{7-\delta}$ crystal, recorded at $2\theta = 13.002°$. The diffraction peaks are superimposed on a background that is the convolution of the energy intensity profile of the radiation on this beamline and the response of the photon detection system. The PbKα peaks in the spectra are from the lead shielding that is used extensively in the beamline hutch.

where κ is the product of Planck's constant and the speed of light. We used the (0,0,11) peak because it was the strongest. Assuming the change in c to be a result of variation in oxygen content, we used Eq. 1 to determine the size of the effect. It is also possible that other systematic changes, such as carbonate invasion, were present in the sample.

Three separate z scans were performed (Fig. 2). The first was made with the beam passing through the central region of the crystal (y = 0 μm), the second with the y position of the sample increased by 20 μm, and the third with y increased an additional 10 μm. The edge of the sample in this direction, as measured with the x-ray beam, was at y = 36 μm. So the last scan (y = 30 μm) came from an area about 6 μm from the lateral face of the crystal.

The value of $7 - \delta$ determined from a separate measurement on a conventional diffractometer with CuKα radiation was about 6.8; this is comparable to the value determined from the interior portion of the sample. The most striking feature of each scan is the precipitous change in $7 - \delta$ near the edges as the crystal moves into and out of the beam. The value of $7 - \delta$ is relatively constant, to within the scatter in the data, throughout the central region, but falls off significantly on either end. For the scan taken closest to the lateral face (y = 30 μm), $7 - \delta$ is also reduced. Whereas the oxygen content was relatively constant throughout the bulk, it dropped off near the surfaces, as if oxygen had "leaked" out of the sample.

The measured fractional change in the c axis length represented by the data in Fig. 2 is about 0.15%. As a test of the validity of the experiment, a high-purity silicon crystal of similar dimensions was examined in the same way. The position of the Si(400) peak was monitored along the 700-μm length of the crystal. The variance in the measured lattice parameter was less than 0.04%, and no systematic changes were observed as the crystal moved into or out of the beam.

We also analyzed the $Ln_{2-x}M_xCuO_{4-y}$ family of superconductors (where Ln is a lanthanide), which is unique among the cuprates because of the unusual symmetry in the doping characteristics between hole and electron carrier materials. Tetravalent doping ($M = Ce^{4+}$; Ln = Pr, Nd, Sm, or Eu) produces the electron carrier material ($T_c \approx 20$ K) for a range of compositions ($0.14 < x < 0.18$). The production of optimal samples for superconductivity is further complicated by the need for a small oxygen defect ($y \approx 0.02$), usually produced by a high-temperature anneal in an inert atmosphere. There are many reports of mixed-phase behavior in the Nd-Ce-Cu-O system. This phenomenon is usually attributed to inhomogeneities in the oxygen content, though recently inhomogeneities in the Ce concentrations have been described (3).

Cava *et al.* (4) investigated the phase diagram of Nd-Ce-Cu-O for polycrystalline samples for nearby stoichiometries and for several points along the $Nd_{2-x}Ce_x$ compositional line. They report that the occurrence of phase instability in polycrystalline samples is primarily the result of incipient melting, caused by processing at too high a temperature. For samples produced by solid-state reactions alone, they found no evidence for phase instability.

Drews *et al.* (5) studied thick single crystals of $Nd_{2-x}Ce_xCuO_{4-y}$ and found clear evidence for phase segregation in the form of sheets of stoichiometric material in the *ab* plane with varying Ce concentration. Although investigators have usually restricted their attention to thin crystals (30 μm), which show sharp superconducting

Fig. 2. Variation of the oxygen parameter, $7 - \delta$, and of the c axis lattice parameter, both as a function of position, z, along the length of the $YBa_2Cu_3O_{7-\delta}$ crystal; scans were made at three different settings in y: (●) near the center at y = 0.00 μm; (■) closer to the lateral face at y = 20 μm; and (▲) within about 6 μm of the face surface at y = 30 μm. **(Inset)** Orientation of crystal.

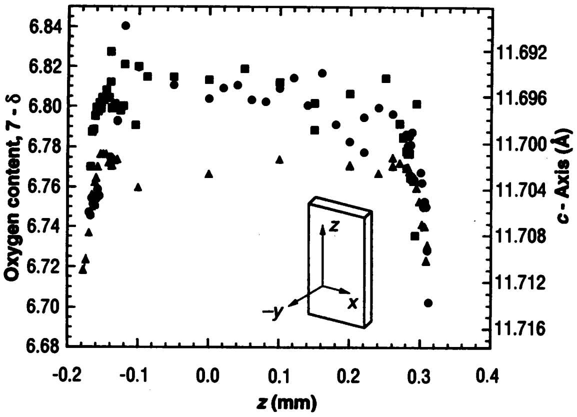

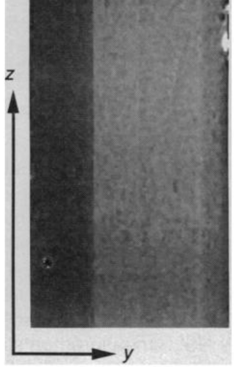

Fig. 3. Photograph of a cross section in the yz plane of the $Nd_{2-x}Ce_xCuO_{4-y}$ crystal.

transitions and behave in accord with Bardeen-Cooper-Schrieffer (BCS) theory, an appreciation of the difficulties present in thicker samples is important. Therefore, we searched for small changes in the c axis lattice parameter in a thick single crystal using a high energy x-ray microprobe. These changes are assumed to be related to variations in the Ce content.

The $Nd_{2-x}Ce_xCuO_{4-y}$ crystal was grown from a CuO flux in an alumina crucible by a directional solidification technique described in detail elsewhere (6). Crystals grown by this method are typically several millimeters on a side and less than 100 μm thick. To induce superconductivity, a post-growth anneal in flowing argon gas at 850°C for 15 hours was required.

Optical microscopic analyses of a polished cross section of the crystal provided the first evidence of an unusual morphology (Fig. 3). When the crystal was viewed between crossed polarizers, variable contrast was observed in the form of stacked layers of material in the ab plane. Four major layers are clearly visible, separated by apparently sharp boundaries without cracks or flux inclusions. Scanning electron microscopy (SEM) coupled with energy-dispersive x-ray spectroscopy (EDXS) measurements across the polished section indicate that the observed optical contrast correlates with a variation in the measured Ce concentration (Fig. 4, open circles). The two inner layers had similar Ce concentrations corresponding to $x = 0.19$, whereas the two outer layers had Ce concentrations corresponding to $x = 0.16$ and 0.13. The ac magnetic susceptibility measured with either orientation of the crystal relative to the pick-up coil showed distinct transitions at 24 and 20 K. The double transitions can be explained if the outer layers correspond to the lower T_c material.

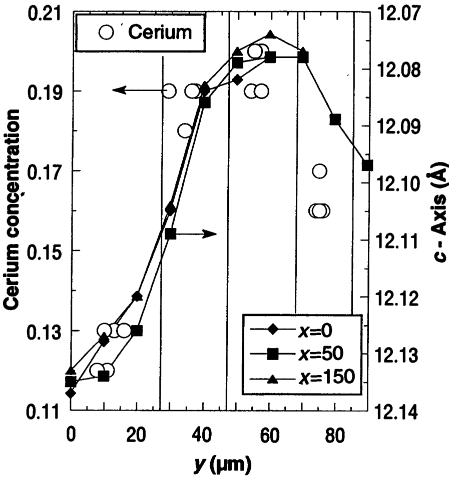

Fig. 4. Variation of the Ce content (○) as measured by EDXS (*6*) and of the c axis lattice parameter (filled symbols) as measured by energy dispersive x-ray diffraction (this work), each as a function of position y, that is, along the c axis of the crystal; scans were made at (◆) $x = 0$, (■) $x = 50$, and (▲) $x = 150$ μm. The errors for the NSLS measurements of the c axis are typically ±0.01 Å. The vertical lines represent the approximate locations of the boundaries between the layers shown in Fig. 3.

Standard diffraction measurements of the $(0,0,6)$ and $(0,0,\bar{6})$ reflections made on a four-circle diffractometer with CuKα radiation confirmed that the c axis lattice parameter was different for each face of the crystal; measured values were 12.082 ± 0.004 and 12.118 ± 0.001 Å. On the basis of the results of Takagi *et al.* (*7*) from powder diffraction studies of this system, these lattice parameters correspond to Ce concentrations of $x = 0.09$ and 0.15, respectively. The interesting morphology of this sample suggests that it is an ideal candidate for study with the high energy x-ray microprobe at NSLS.

The $Nd_{2-x}Ce_xCuO_{4-y}$ crystal was also in the approximate shape of a rectangular solid, with dimensions 3 mm by 1.5 mm by 80 μm. It was mounted on the ω,χ circle in the same manner as described above. Spectra were recorded as a function of y every 10 μm for three different x positions ($x = 0$, 50, and 150 μm). At each setting, the crystal first was centered in ω and χ, and then the spectrum was recorded. The peak energies for the even-order $(0,0,\ell)$ reflections were measured (mixed-order reflections are excluded by symmetry for this structure) and used to calculate the c-axis lattice parameter (Fig. 4).

There is a general similarity of shape in the Ce content variation across the edge of the crystal as measured by EDXS and the variation of c axis parameter measured at NSLS. If the variation in the c axis is interpreted as a variation of Ce content, according to the dependence determined by Takagi *et al.* (*7*), then the data show a variation from $x = 0.12$ at one face, to $x = 0.16$ for the interior region, to $x = 0.07$ near the opposite face. This is similar to the variation determined by EDXS. Furthermore, because the wiggler synchrotron source produces hard x-rays that can penetrate deeply into the sample, we have evidence of Ce variation that is not restricted to the surface. Microstructural variations on the scale of 10 or 20 μm are clearly visible in the NSLS data.

These observations are direct evidence of subtle structural modifications on this spatial scale. The two high-T_c single-crystal superconductors examined in this investigation were probed with an extremely intense x-ray beam only 5 μm by 10 μm in cross section. For both crystals, the data reveal small structural variations on a spatial scale of 10 to 20 μm. For the $YBa_2Cu_3O_{7-\delta}$, the observed effect is believed to result from an apparent loss of oxygen near the surfaces. In the case of $Nd_{2x}Ce_xCuO_{4-y}$, the observed structural variances are interpreted in terms of changes in the Ce content. These results emphasize the need for caution in the interpretation of experimental results for HTS.

There are two length scales that characterize the superconducting state: the penetration depth, λ, and the coherence length, ξ. In HTS, both are highly anisotropic and change by an order of magnitude in going from the ab plane to the c direction. At 0 K, λ_{ab} is of the order of 1000 Å, whereas λ_c is 10 times greater; ξ_{ab} is of the order of 10 Å, whereas ξ_c is only one-tenth as large. Although the length scales probed here are large compared with these values, the observed inhomogeneities are big enough to alter the properties measured in standard measurements. In particular, experiments that depend on clean surfaces with uniform, ideal, superconducting properties, such as penetration depth and tunneling, will be affected strongly by such structural features. This may be particularly true for $YBa_2Cu_3O_{7-\delta}$ crystals (*8*). On the other hand, thin $Nd_{2-x}Ce_xCuO_{4-y}$ crystals (<20 μm) exhibit no evidence of structural inhomogeneities. This point is highlighted by tunneling and penetration-depth measurements on thin, single-phase $Nd_{2-x}Ce_xCuO_{4-y}$ crystals, which produce results consistent with BCS theory (*9*, *10*).

As we strive to achieve smaller beam sizes, we are likely to observe significant structural defects in submicrometer length scales. Ideally, as our resolution increases, we will be able to answer more subtle questions regarding the nature of the defect structures and their origins.

REFERENCES AND NOTES

1. T. A. Vanderah *et al.*, *J. Cryst. Growth* **118**, 385 (1992).
2. J. Giapintzakis, D. M. Ginsberg, P.-D. Han, *J. Low Temp. Phys.* **77**, 155 (1989).
3. W. Sadowski *et al.*, *J. Less-Common Met.* **164**, **165**, 824 (1990).
4. R. J. Cava *et al.*, *Phys. C* **199**, 65 (1992). In this paper, a variation of the diffraction angle for the (006) peak with Ce content is reported on the basis of data taken with monochromatic x-rays (wavelength λ = 1.19996 Å). However, the resulting c axis length is inconsistent with the accepted value. After private discussions with one of the authors, it was agreed that an alternate wavelength calibration (λ = 1.20526 Å) may be appropriate.
5. A. R. Drews *et al.*, *Phys. C* **200**, 122 (1992).
6. J. L. Peng, Z. Y. Li, R. L. Greene, *ibid.* **177**, 79 (1991).
7. H. Takagi, S. Uchida, Y. Tokura, *Phys. Rev. Lett.* **62**, 1197 (1989).
8. W. N. Hardy, D. A. Bonn, D. C. Morgan, R. Liang, K. Zhang *ibid.* **70**, 3999 (1993).
9. S. M. Anlage *et al.*, in preparation.
10. Q. Huang *et al.*, *Nature* **347**, 369 (1990).
11. A.R.D. acknowledges the support of the Office of Naval Technology. Work performed by the group from the University of Maryland was supported in part by the National Science Foundation under grant DMR 9209668. The work was also supported in part by the Office of Naval Research. We are grateful to H. Hoff for helpful technical discussions and to Z. Y. Li for help in preparation of the $Nd_{2-x}Ce_xCuO_{4-y}$ crystals.

9 November 1993; accepted 21 January 1994